# Supplementary Information for

# The organization of two new cortical interneuronal circuits

Xiaolong Jiang[1,4], Guangfu Wang[1,4], Alice J. Lee[1,3], Ruth L. Stornetta[1] & J. Julius Zhu[1,2]

Departments of Pharmacology[1], Neuroscience[2], and Biology[3], School of Medicine and College of Arts and Sciences, University of Virginia, Charlottesville, VA 22908

**Figure S1**

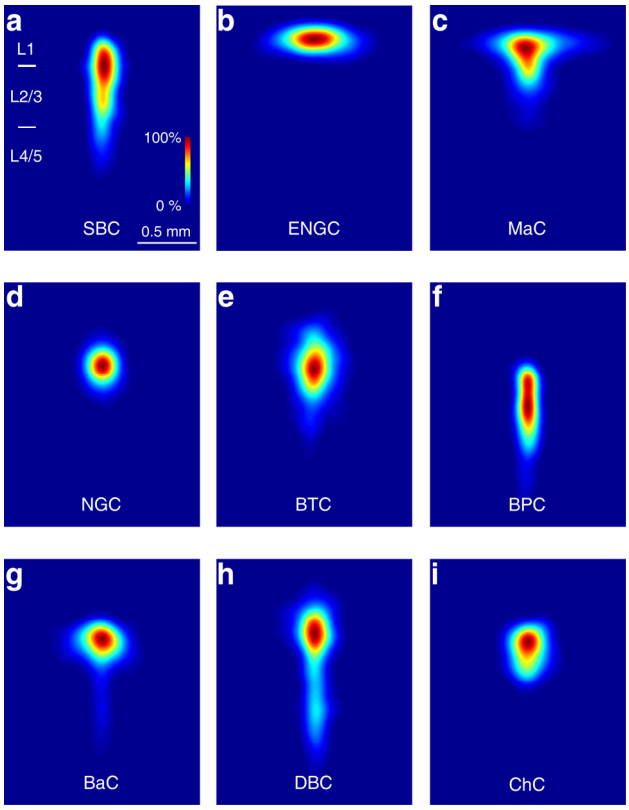


**Fig. S1. Axonal length density maps of L1-3 interneurons.**
**(a-i)** Axonal length density maps of L1 interneurons (SBC: *n*=17; ENGC: *n*=15) and L2/3 interneurons (MaC: *n*=15; NGC: *n*=28; BTCs: *n*=19; BPC: *n*=15; BaC: *n*=15; DBC: *n*=16; ChC: *n*=15).

**Figure S2**

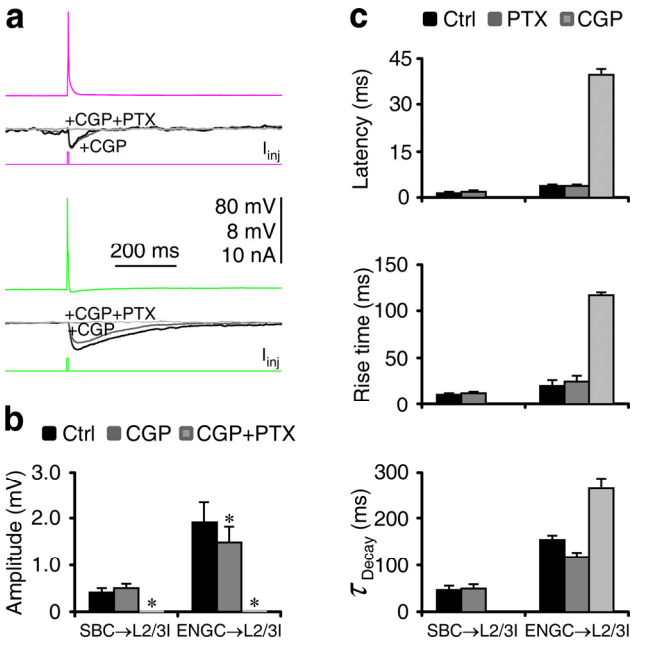


**Fig. S2. SBCs and ENGCs form inhibitory circuits with different kinetics and GABA-R compositions.**
**(a)** SBC- and ENGC-evoked uIPSPs in L2/3 interneurons from acute cortical slices before (black traces) and after (gray traces) bath application of 5 µM CGP35348, which blocks $GABA_B$ receptors, and 100 µM picrotoxin (PTX), which blocks $GABA_A$ receptors. Scale bars apply to all recording traces with 80 mV and 8 mV bars applied to traces with and without action potentials, respectively.
**(b)** The bar graphs show the amplitudes of SBC- and ENGC-evoked uIPSPs before and after bath application of CGP and PTX. Values for SBC-evoked uIPSPs (Ctrl: 0.41±0.10 mV; CGP: 0.48±0.09 mV; *n*=12, $Z$=2.5; *p*=0.08; CGP+PTX: 0.00±0.00 mV; *n*=12, $Z$=2.8; *p*<0.0005) and ENGC-evoked uIPSPs (Ctrl: 1.93±0.42 mV; CGP: 1.49±0.33 mV; *n*=8, $Z$=2.5; *p*<0.05; CGP+PTX: 0.00±0.00 mV; *n*=8, $Z$=2.6; *p*<0.0005). Asterisks indicate *p*<0.05 (Wilcoxon tests).
**(c)** The bar graphs show the latencies, rise times and decay time constants of PTX- and CGP35348-sensitive uIPSPs in L2/3 interneurons (SBC→MaC: *n*=1; SBC→NGCs: *n*=3; SBC→BTC: *n*=4; SBC→BPC: *n*=1; SBC→BaC: *n*=1; SBC→DBC: *n*=1; SBC→ChC: *n*=1; ENGC→MaC: *n*=1; ENGC→NGCs: *n*=3; ENGC→BTC: *n*=4). Values for the latencies (Ctrl: 1.5±0.2 ms; PTX: 1.8±0.3 ms; *n*=12 for SBC-evoked uIPSPs; Ctrl: 3.9±0.5 ms; PTX: 3.8±0.4 ms; CGP: 39.5±1.6 ms; *n*=8 for ENGC-evoked uIPSPs), rise times (Ctrl: 11.2±1.4 ms; PTX: 12.4±2.0 ms; *n*=12 for SBC-evoked uIPSPs; Ctrl: 20.3±2.5 ms; PTX: 25.1±5.1 ms; CGP: 116.3±2.6 ms; *n*=8 for ENGC-evoked uIPSPs), and decay time constants (Ctrl: 41.3±5.5 ms; PTX: 40.3±3.7 ms; *n*=12 for SBC-evoked uIPSPs; Ctrl: 154.3±6.1 ms; PTX: 115.9±9.1 ms; CGP: 262.2±22.1 ms; *n*=8 for ENGC-evoked uIPSPs). Note that CGP- and PTX-sensitive uIPSPs were calculated by digitally subtracting the evoked responses after including additional CGP and PTX in the bath solution, respectively.

**Figure S3**

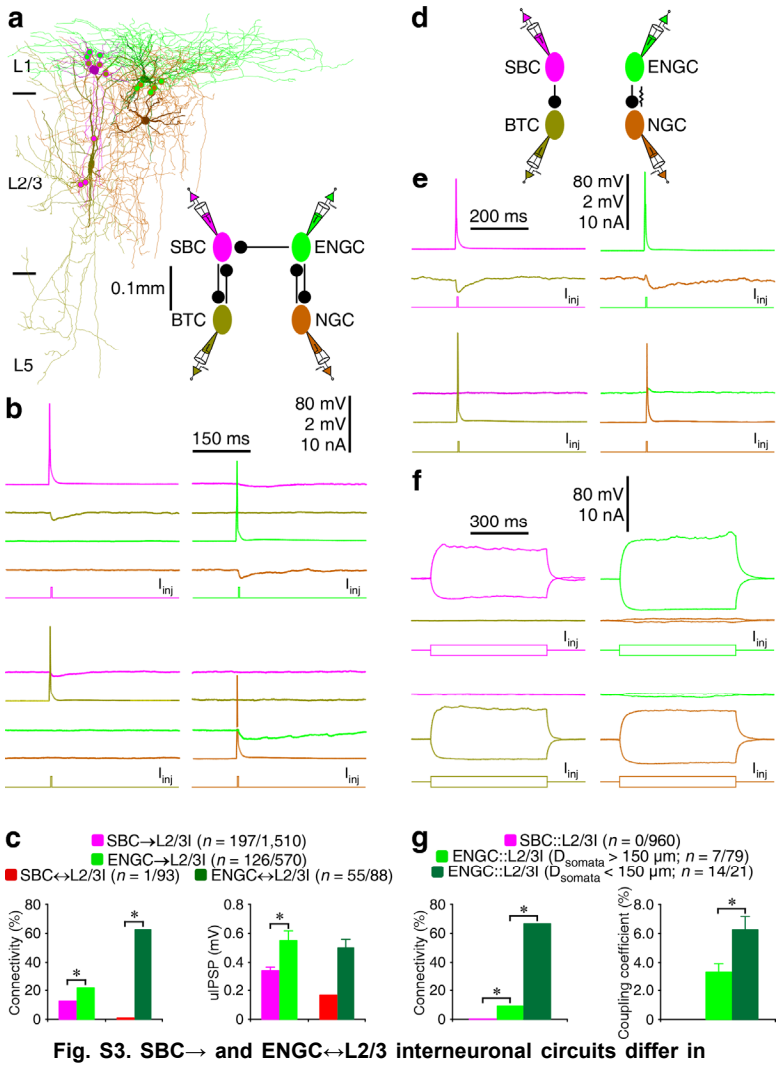


**Fig. S3. SBC→ and ENGC↔L2/3 interneuronal circuits differ in synaptic connectivity.**

**(a)** Reconstruction of L1 SBC (pink), L1 ENGC (green), L2/3 BTC (yellow) and L2/3 NGC (brown) recorded simultaneously from an acute cortical slice. The double colored dots indicate the putative synaptic contacts. The schematic drawing shows symbolically their synaptic connections.
**(b)** Single action potentials elicited in presynaptic L1-3 interneurons evoked uIPSPs in postsynaptic L1-3 interneurons.
**(c)** The bar graphs show the connectivity and strength of synapses formed between L1-3 interneurons located within the same column. Values for the connectivity (SBC→L2/3I: 13.0%, $n$=197 of 1510 tested connections; ENGC→L2/3I: 22.1%, $n$=126 of 570 tested connections; $\chi^2$=25.9; $p$<0.0005; SBC↔L2/3I: 1.1%, $n$=1 of 93 tested SBC→L2/3I pairs; ENGC↔L2/3I: 62.5%, $n$=55 of 88 tested ENGC→L2/3I pairs; $\chi^2$=79.8; $p$<0.0005; Chi-squared tests), and strength (SBC→L2/3I: 0.34±0.03 mV, $n$=128; ENGC→L2/3I: 0.54±0.07 mV, $n$=80; $U$=3,499; $p$<0.005; Mann-Whitney Rank Sum test; L2/3I→SBC: 0.17 mV, $n$=1 SBC↔L2/3I pair; L2/3I→ENGC: 0.50±0.06 mV, $n$=53 ENGC↔L2/3I pairs).
**(d)** The schematic drawing shows symbolically inhibitory connections between SBC and BTC, and inhibitory and electric connections between ENGC and NGC recorded from an acute cortical slice.
**(e)** The recording traces show that single action potentials elicited in presynaptic SBC evoked uIPSPs in postsynaptic BTC, single action potentials elicited in presynaptic ENGC evoked spikelets and uIPSPs in postsynaptic NGC, and single action potentials elicited in NGC evoked spikelets in postsynaptic ENGC.
**(f)** The recording traces show that the depolarizing and hyperpolarizing current injections in SBC and BTC had no effect on the membrane potentials of BTC and SBC, respectively, and the current injections in ENGC and NGC induced small membrane depolarization and hyperpolarization in NGC and ENGC, respectively. Scale bars in **b**, **e** and **f** apply to all recording traces with 80 mV and 2 mV bars applied to traces with and without action potentials, respectively.
**(g)** The bar graphs show the connectivity and coupling coefficient of electric synapses formed between L1 and L2/3 interneurons. Values for the electric synapse connectivity (SBC::L2/3I: 0.0%, $n$=0 of 960 tested pairs; ENGC::L2/3I: 9.1%, $n$=7 of 79 tested pairs with intersomatic distance >150 µm; $\chi^2$=85.6; $p$<0.0005; ENGC::L2/3I: 66.7%, $n$=14 of 21 tested pairs with intersomatic distance <150 µm; $\chi^2$=649.3; $p$<0.0005; Chi-squared tests), and coupling coefficient (ENGC::L2/3I: 3.30±0.59%, $n$=7 pairs with intersomatic distance >150 µm; ENGC::L2/3I: 6.22±0.91%, $n$=14 pairs with intersomatic distance <150 µm; $U$=77.0; $p$<0.05; Mann-Whitney Rank Sum test). Asterisks in **c** and **g** indicate $p$<0.05 (Chi-squared or Mann-Whitney Rank Sum tests).

**Figure S4**

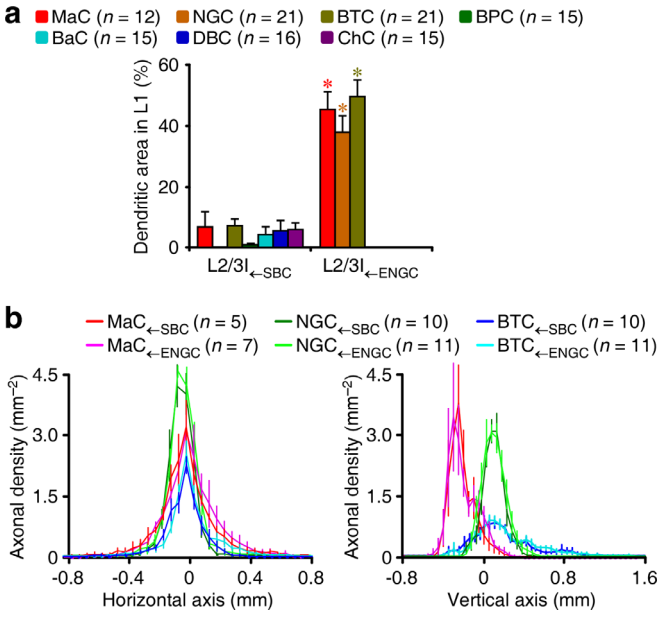


**Fig. S4. L2/3 interneurons in SBC→ and ENGC↔L2/3 interneuronal circuits differ in dendritic anatomy.**
**(a)** L1 fractions of dendritic arborization of L2/3 interneurons targeted by SBCs and ENGCs (MaC$_{\leftarrow SBC}$: 6.5±5.1%, $n$=5; MaC$_{\leftarrow ENGC}$: 45.5±5.6%, $n$=7; $U$=0.0; $p$<0.005; NGC$_{\leftarrow SBC}$: 0.0±0.0%, $n$=10; NGC$_{\leftarrow ENGC}$: 37.8±5.8%, $n$=11; $U$=0.0; $p$<0.0001; BTC$_{\leftarrow SBC}$: 7.0±2.2%, $n$=10; BTC$_{\leftarrow ENGC}$: 49.7±5.2%, $n$=11; $U$=0.0; $p$<0.0001; BPC: 0.9±0.3%, $n$=15; BaC: 4.3±2.1%, $n$=15; DBC: 5.4±3.2%, $n$=16; ChC: 6.0±1.9%, $n$=15). Asterisks indicate $p$<0.05 (Mann-Whitney Rank Sum tests).
**(b)** Axonal length density plots targeted by SBCs and ENGCs (MaC$_{\leftarrow SBC}$: $n$=5; MaC$_{\leftarrow ENGC}$: $n$=7; $F$=0.4; $p$>0.05; NGC$_{\leftarrow SBC}$: $n$=10; NGC$_{\leftarrow ENGC}$: $n$=11; $F$=1.8; $p$>0.05; BTC$_{\leftarrow SBC}$: $n$=10; BTC$_{\leftarrow ENGC}$: $n$=11; $F$=2.7; $p$>0.05; ANOVA tests). Mann-Whitney Rank Sum tests indicate that the soma of MaCs, NGCs and BTCs targeted by SBCs were located deeper in L2/3 than that of MaCs, NGCs and BTCs targeted by ENGCs (MaC$_{\leftarrow SBC}$: 161.8±19.9 µm; $n$=5; MaC$_{\leftarrow ENGC}$: 76.0±8.3 µm; $n$=7; $U$=0.0; $p$<0.05; NGC$_{\leftarrow SBC}$: 166.7±17.8 µm; $n$=10; NGC$_{\leftarrow ENGC}$: 44.2±6.0 µm; $n$=11; $U$=0.0; $p$<0.01; BTC$_{\leftarrow SBC}$: 161.3±22.4 µm; $n$=10; BTC$_{\leftarrow ENGC}$: 66.3±5.0 µm; $n$=11; $U$=0.0; $p$<0.01).

**Figure S5**

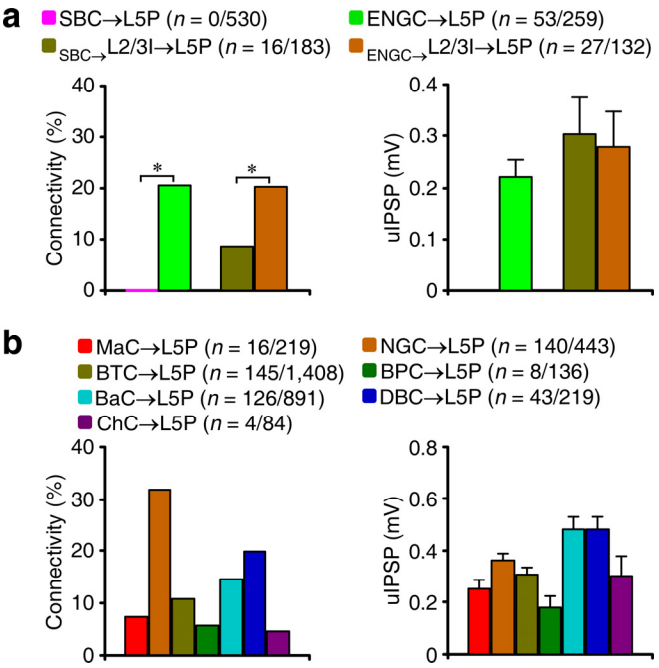


**Fig. S5. SBC→ and ENGC↔L2/3I interneuronal circuits differentially innervate L5 pyramidal neurons.**
**(a)** The bar graphs show the connectivity and strength of synapses formed between SBCs, ENGCs, L2/3 interneurons postsynaptic to SBCs, or L2/3 interneurons postsynaptic to ENGCs, and L5 pyramidal neurons within the same column. Values for the connectivity (SBC→L5P: 0.0%, $n$=0 of 530 tested connections; ENGC→L5P: 20.4%, $n$=53 of 259 tested connections; $\chi^2$=116.3; $p$<0.005; $_{SBC\rightarrow}$L2/3I→L5P: 8.7%, $n$=16 of 183 tested connections; $_{ENGC\leftrightarrow}$L2/3I→L5P: 20.5%, $n$=27 of 132 tested connections; $\chi^2$=8.8; $p$<0.005; Chi-squared tests) and strength (ENGC→L5P: 0.22±0.03 mV, $n$=19; $_{SBC\rightarrow}$L2/3I→L5P: 0.30±0.07 mV, $n$=15; $_{ENGC\leftrightarrow}$L2/3I→L5P: 0.28±0.07 mV, $n$=15; $U$=115.0; $p$=0.92; Mann-Whitney Rank Sum test). Note that ENGCs, but not L2/3 interneurons postsynaptic to ENGCs, form synapses on L5 pyramidal neurons located in both the same and neighboring columns (ENGC→L5P$_{\text{same column}}$: 20.4%, $n$=53/259; ENGC→L5P$_{\text{neighboring column}}$: 5.2%, $n$=6/116; $\chi^2$=14.1; $p$<0.005; $_{ENGC\leftrightarrow}$MaC→L5P$_{\text{same column}}$: 7.1%, $n$=1/14; $_{ENGC\leftrightarrow}$MaC→L5P$_{\text{neighboring column}}$: 0.0%, $n$=0/14; $\chi^2$=1.0; $p$=0.301; $_{ENGC\leftrightarrow}$NGC→L5P$_{\text{same column}}$: 33.3%, $n$=17/51; $_{ENGC\leftrightarrow}$NGC→L5P$_{\text{neighboring column}}$: 0.0%, $n$=0/23; $\chi^2$=10.0; $p$<0.005; $_{ENGC\leftrightarrow}$BTC→L5P$_{\text{same column}}$: 15.8%, $n$=9/57; $_{ENGC\leftrightarrow}$BTC→L5P$_{\text{neighboring column}}$: 0.0%, $n$=0/23; $\chi^2$=4.1;

$p$<0.05; Chi-squared tests). Asterisks indicate $p$<0.05 (Chi-squared tests).
**(b)** The bar graphs show the connectivity and strength of synapses formed between L2/3 interneurons and L5 pyramidal neurons within the same column. Values for the strength (MaC→L5P: 0.24±0.03 mV, $n$=11; NGC→L5P: 0.35±0.03 mV, $n$=88; BTC→L5P: 0.30±0.03 mV, $n$=89; BPC→L5P: 0.17±0.04 mV, $n$=8; BaC→L5P: 0.47±0.05 mV, $n$=67; DBC→L5P: 0.47±0.05 mV, $n$=41; ChC→L5P: 0.29±0.07 mV, $n$=4; $F$=3.8; $p$<0.005; ANOVA test). Note that L2/3 interneurons form synapses on L5 pyramidal neurons located in the same columns, but not those in neighboring columns (MaC→$L5P_{same\ column}$: 7.3%, $n$=16/219; MaC→$L5P_{neighboring\ column}$: 0.0%, $n$=0/74; $\chi^2$=5.7; $p$<0.05; NGC→$L5P_{same\ column}$: 31.6%, $n$=140/443; NGC→$L5P_{neighboring\ column}$: 0.0%, $n$=0/37; $\chi^2$=16.5; $p$<0.005; BTC→$L5P_{same\ column}$: 10.3%, $n$=145/1,408; BTC→$L5P_{neighboring\ column}$: 0.0%, $n$=0/106; $\chi^2$=11.8; $p$<0.005; BPC→$L5P_{same\ column}$: 4.6%, $n$=8/136; BPC→$L5P_{neighboring\ column}$: 0.0%, $n$=0/81; $\chi^2$=4.9; $p$<0.05; BaC→$L5P_{same\ column}$: 14.1%, $n$=126/891; BaC→$L5P_{neighboring\ column}$: 0.0%, $n$=0/51; $\chi^2$=8.3; $p$<0.05; DBC→$L5P_{same\ column}$: 19.6%, $n$=43/219; DBC→$L5P_{neighboring\ column}$: 0.0%, $n$=0/43; $\chi^2$=19.1; $p$<0.005; ChC→$L5P_{same\ column}$: 4.8%, $n$=4/84; $p$<0.005; ChC→$L5P_{neighboring\ column}$: 0.0%, $n$=0/76; $\chi^2$=3.7; $p$<0.05; Chi-squared tests).

**Figure S6**

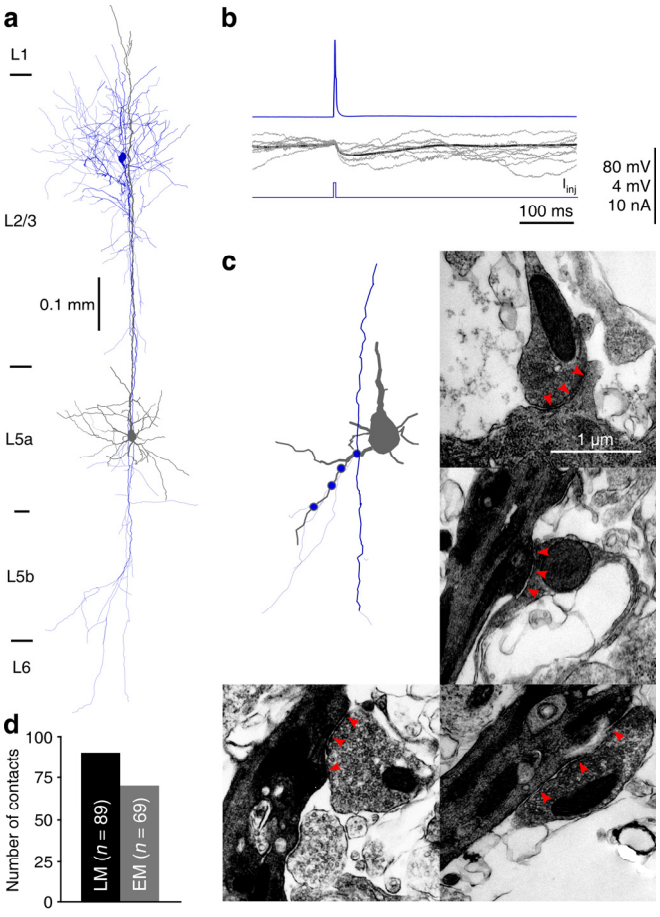


**Fig. S6. EM confirms the majority of LM-identified synaptic boutons.**
**(a)** Reconstruction of L2/3 DBC (blue) and L5 pyramidal neuron (grey) recorded simultaneously from an acute cortical slice. The double colored dots indicate the putative synaptic contacts identified by LM.
**(b)** Single action potentials elicited in presynaptic DBC evoked uIPSPs in postsynaptic L5 pyramidal neuron. 80 mV and 4 mV bars apply to traces with and without action potentials, respectively. Note the average uIPSP trace (black), as well as superimposed individual uIPSP traces (gray).
**(c)** Four light microscopy (LM)-identified synaptic boutons were confirmed with electron microscopy (EM). Arrow heads in EM images indicate synaptic junctions established by the axon of DBC.
**(d)** The numbers of LM- and EM-identified synapses.

**Figure S7**

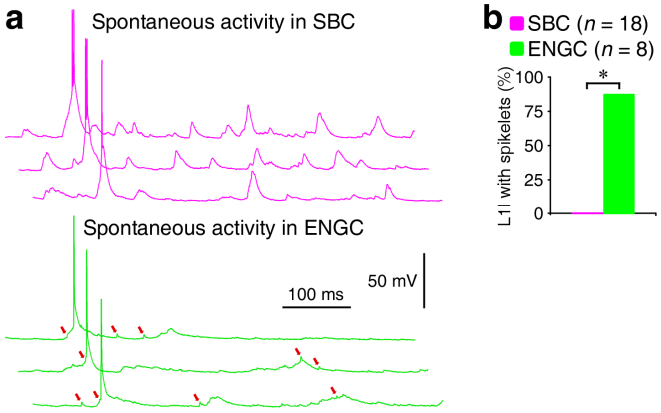


**Fig. S7. Spikelet-like events are prevalent in ENGCs recorded *in vivo*.**
**(a)** Spontaneous recording traces of the SBC and ENGC in figure 8a-b in expanded scales. Red arrows indicate the spikelets characteristic of electric synapses. Note the spikelets absent in SBC, but prevalent in ENGC. Scale bars apply to all recording traces.
**(b)** Percentages of L1 interneurons displayed the spikelets (SBCs: 0%, $n$=0/18; ENGCs: 87.5%, $n$=7/8; $\chi^2$=21.6). Asterisk indicates $p$<0.05 (Chi-squared test).

**Figure S8**

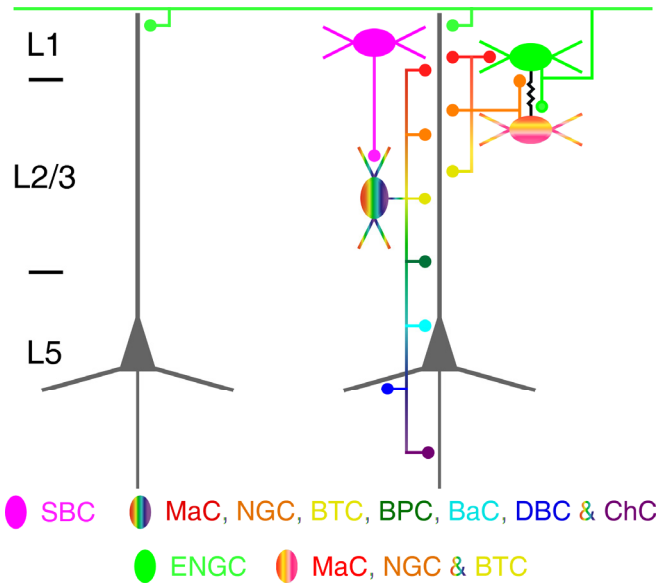


**Fig. S8. Schematic drawing shows key features of SBC→ and ENGC↔L2/3I→L5 pyramidal neuronal circuits.**
See the main text for the detailed architecture of the two cortical interneuronal circuits.

## Table S1

Synaptic connectivity between L1 and L2/3 interneurons

| Cell connection pattern | L2/3Is in same columns (Connected/tested and %) | | L2/3Is in neighboring columns (Connected/tested and %) | | $\chi^2$ and *P* value (Chi-squared) | |
|---|---|---|---|---|---|---|
| SBC→MaC | 6/124 | 4.8% | 0/79 | 0.0% | 3.9 | 0.047 |
| SBC→NGC | 18/250 | 7.3% | 0/69 | 0.0% | 5.3 | 0.022 |
| SBC→BTC | 68/466 | 14.6% | 0/76 | 0.0% | 12.7 | 0.000 |
| SBC→BPC | 34/122 | 27.9% | 0/19 | 0.0% | 7.0 | 0.008 |
| SBC→BaC | 29/305 | 9.5% | 0/64 | 0.0% | 6.6 | 0.012 |
| SBC→DBC | 7/82 | 8.5% | 0/43 | 0.0% | 3.9 | 0.048 |
| SBC→ChC | 13/75 | 17.3% | 0/22 | 0.0% | 4.4 | 0.036 |
| ENGC→MaC | 11/60 | 18.3% | 1/18 | 5.5% | 1.7 | 0.188 |
| ENGC→NGC | 46/108 | 42.6% | 3/22 | 13.2% | 6.5 | 0.011 |
| ENGC→BTC | 62/192 | 32.3% | 4/27 | 14.8% | 3.4 | 0.064 |
| ENGC→BPC | 0/34 | 0.0% | 0/7 | 0.0% | -- | |
| ENGC→BaC | 0/119 | 0.0% | 0/23 | 0.0% | -- | |
| ENGC→DBC | 0/31 | 0.0% | 0/11 | 0.0% | -- | |
| ENGC→ChC | 0/17 | 0.0% | 0/4 | 0.0% | -- | |

| Cell connection pattern | SBCs (Connected/tested and %) | | ENGCs (Connected/tested and %) | | $\chi^2$ and *P* value (Chi-squared) | |
|---|---|---|---|---|---|---|
| MaC→L1I | 43/109 | 39.4% | 27/49 | 55.1% | 3.4 | 0.067 |
| NGC→L1I | 41/152 | 27.0% | 41/79 | 51.9% | 14.1 | 0.000 |
| BTC→L1I | 9/282 | 3.2% | 19/126 | 15.1% | 19.3 | 0.003 |
| BPC→L1I | 0/58 | 0.0% | 0/18 | 0.0% | -- | |
| BaC→L1I | 1/174 | 0.6% | 4/72 | 5.6% | 6.3 | 0.012 |
| DBC→L1I | 0/60 | 0.0% | 0/25 | 0.0% | -- | |
| ChC→L1I | 0/36 | 0.0% | 0/18 | 0.0% | -- | |
| MaC↔L1I | 0/43 | 0.0% | 9/27 | 33.3% | 16.4 | 0.000 |
| NGC↔L1I | 0/41 | 0.0% | 30/41 | 73.2% | 47.3 | 0.000 |
| BTC↔L1I | 1/9 | 11.1% | 15/19 | 79.9% | 11.5 | 0.000 |

Note that SBCs rarely form mutual inhibitory connections with L2/3 MaCs, NGCs and BTCs, even though many of which, presumably interconnected with ENGCs, inhibit SBCs.

## Table S2

Correlation of physiology-, LM- and EM-identified inhibitory connections on L5 pyramidal neurons

| Cell connection pattern | Connected pairs (LM/physiology) | No. of boutons in LM-identified pairs | Unconnected pairs (LM/physiology) | $\chi^2$ and *P* value* (Chi-squared) | |
|---|---|---|---|---|---|
| ENGC→L5P | 6/7 | 4.5±0.7 (*n*=6) | 11/11 | 1.7 | 0.729 |
| MaC→L5P | 10/11 | 5.4±0.4 (*n*=10) | 14/14 | 1.3 | 0.774 |
| NGC→L5P | 17/17 | 3.7±0.3 (*n*=17) | 29/30 | 0.6 | 0.831 |
| BTC→L5P | 27/28 | 5.7±0.6 (*n*=27) | 71/71 | 2.6 | 0.874 |
| BPC→L5P | 8/8 | 4.3±0.4 (*n*=8) | 14/14 | -- | 1.000 |
| BaC→L5P | 28/31 | 3.8±0.3 (*n*=26) | 42/43 | 1.9 | 0.501 |
| DBC→L5P | 26/27 | 4.1±0.3 (*n*=26) | 24/24 | 0.9 | 0.843 |
| ChC→L5P | 4/4 | 3.8±0.6 (*n*=4) | 10/10 | -- | 1.000 |

| Cell connection pattern | No. of cell pairs | No. of LM-identified synapses | No. of EM-identified synapses | Confirmation rate (%) |
|---|---|---|---|---|
| MaC→L5P | 1 | 6 | 5 | 83.3% |
| NGC→L5P | 6 | 38 | 26 | 68.4% |
| BTC→L5P | 3 | 18 | 15 | 83.3% |
| BPC→L5P | 1 | 4 | 3 | 75.0% |
| BaC→L5P | 4 | 19 | 16 | 84.2% |
| DBC→L5P | 1 | 4 | 4 | 100.0% |
| Total | 15 | 89 | 69 | 77.5% |

*Note the Chi-squared tests show no difference between physiologically and light microscopically identified synaptic connections formed between various types of L1-3 interneurons and L5 pyramidal neurons.

## Table S3

Synaptic connectivity and strength between L1 and L2/3 interneurons in different cortical areas

| Presynaptic cell type | L2/3Is in sensory cortex (Connected/tested and %) | | L2/3Is in motor cortex (Connected/tested and %) | | $\chi^2$ and *P* value (Chi-squared) | |
|---|---|---|---|---|---|---|
| SBC | 110/801 | 13.7% | 52/469 | 11.1% | 1.9 | 0.171 |
| ENGC | 40/186 | 21.5% | 16/77 | 20.8% | 0.0 | 0.895 |

| Presynaptic cell type | L2/3Is in sensory cortex (mV) | L2/3Is in motor cortex (mV) | *U and P* value (M-W Rank Sum) | |
|---|---|---|---|---|
| SBC | 0.34±0.04 (*n*=110) | 0.35±0.05 (*n*=52) | 858 | 0.115 |
| ENGC | 0.68±0.10 (*n*=40) | 0.60±0.14 (*n*=16) | 370 | 0.080 |

## Table S4

Synaptic connectivity and strength between L1-3Is and L5 pyramidal neurons in different cortical areas

| Presynaptic cell type | L5Ps in sensory cortex (Connected/tested and %) | | L5Ps in motor cortex (Connected/tested and %) | | $\chi^2$ and *P* value (Chi-squared) | |
|---|---|---|---|---|---|---|
| MaC | 7/112 | 6.3% | 5/83 | 6.0% | 0.0 | 0.791 |
| NGC | 88/279 | 31.5% | 30/99 | 30.3% | 0.1 | 0.819 |
| BTC | 82/831 | 9.9% | 30/319 | 9.4% | 0.1 | 0.812 |
| BPC | 3/66 | 4.5% | 1/26 | 3.9% | 0.0 | 0.882 |
| BaC | 72/507 | 14.2% | 31/238 | 13.0% | 0.2 | 0.662 |
| DBC | 23/127 | 18.1% | 13/63 | 20.6% | 0.2 | 0.676 |
| ChC | 2/44 | 4.5% | 1/19 | 5.3% | 0.0 | 0.902 |
| ENGC | 13/72 | 18.1% | 9/49 | 18.3% | 0.0 | 0.965 |

| Presynaptic cell type | L5Ps in sensory cortex (mV) | L5Ps in motor cortex (mV) | *U and P* value (M-W Rank Sum) | |
|---|---|---|---|---|
| MaC | 0.25±0.06 (*n*=7) | 0.22±0.04 (*n*=5) | 14 | 0.931 |
| NGC | 0.42±0.06 (*n*=88) | 0.39±0.06 (*n*=30) | 1,048 | 0.268 |
| BTC | 0.30±0.06 (*n*=82) | 0.29±0.03 (*n*=30) | 1,111 | 0.492 |
| BPC | 0.18±0.10 (*n*=3) | 0.14 (*n*=1) | -- | |
| BaC | 0.51±0.10 (*n*=72) | 0.49±0.12 (*n*=31) | 975 | 0.484 |
| DBC | 0.59±0.11 (*n*=23) | 0.47±0.07 (*n*=13) | 135 | 0.553 |
| ChC | 0.24 (*n*=2) | 0.26 (*n*=1) | -- | |
| ENGC | 0.25±0.04 (*n*=13) | 0.26±0.06 (*n*=9) | 54 | 0.690 |

**Movie S1. 3D reconstruction reveals distinguished axonal anatomy of SBCs and ENGCs.**
This movie shows the 3D structure of L1 SBC (pink) and L1 ENGC (green) recorded from an acute cortical slice.

**Movie S2. 3D reconstruction reveals distinguished axonal anatomy of L2/3 interneurons.**
This movie shows the 3D structure of L2/3 MaC (red), NGC (orange), BTC (yellow), BPC (dark green), BaC (cyan), DBC (blue) and ChC (purple) recorded from acute cortical slices.